

Microwave liquid-crystal variable phase grating

Fuzi Yang

Liquid Crystal Research Centre, Department of Chemistry, Tsinghua University, Beijing 100084, China

J. R. Sambles^{a)}

Thin Film Photonics, School of Physics, University of Exeter, Exeter EX4 4QL, England

(Received 5 January 2004; accepted 30 June 2004)

A voltage-controlled variable phase grating, at microwave frequencies, is described and its response characterized. It comprises a stack of 71 aluminium strips of 1 mm thickness separated by 75 μm spaces, filled with aligned nematic liquid crystal. For microwaves polarized normal to the grating strips there are a set of resonant transmitted frequencies. By varying the voltages applied across the liquid crystal layers and their distribution, a variable phase microwave grating is realized. This allows low-voltage control of output beam profile and intensity. © 2004 American Institute of Physics. [DOI: 10.1063/1.1787898]

In a wide range of applications the use of microwave devices has increased significantly in recent years. The requirement for compact, low cost, low voltage, and low power consumption microwave modulation devices has, therefore, also grown. Concurrently there has been the burgeoning use of low voltage, low power consumption displays whose functioning depends on the elasticity and high birefringence of thermotropic liquid crystals. While this birefringence extends beyond the visible into the microwave regime,¹ only a few microwave devices using liquid crystals, for example, microstrip line¹ or waveguide²⁻⁴ structures, have been reported.

Recently, however, a phenomenon, which shows strongly enhanced transmission of electromagnetic radiation through thin, periodic metallic samples containing very small hole arrays^{5,6} or thicker samples having narrow slits,^{7,8} has been demonstrated. Both have been attributed to⁷ the resonant coupling of surface plasmon polaritons (SPPs). For the narrow slit structures, the evanescent fields of SPPs on each side of a single groove form coupled SPPs which set up standing waves leading to large field enhancements within the grooves^{9,10} and strong transmission. This resonant transmission through deep narrow grooves in metallic structures has now been reported for microwaves.¹¹ By combining this metallic slat grating structure with liquid crystals by filling the grooves with voltage-controllable aligned liquid crystal we have demonstrated a microwave voltage-controlled wavelength selector.¹² (Even a single slit¹³ shows quite strong transmission for waves polarized with their E field perpendicular to the slit.) The “extraordinary transmission” observed for an array of such metallic slits, a deep grating, is the result of constructive interference of the emission of radiation from the Fabry-Perot-like resonances localized in each cavity. Provided the frequency width of the modes is sufficient then by changing the microwave path length in separate cavities, by voltage control of the liquid crystal placed within such slits, it should be possible to control the relative phase of the emission from each cavity. Then for any chosen wavelength the transmission from the grating can be flexibly controlled by constructive interference of the trans-

mission, with different intensities and phases from different slits.

In this letter, we demonstrate a voltage-controlled liquid crystal variable phase grating at microwave frequencies. The grating geometry (Fig. 1) comprises a stack of 71 strips of aluminium with mylar spacers at each end. These 70 gaps are divided into seven groups of ten gaps in each group. An ac source (1 kHz) is used to apply different voltages independently to each gap within one group with the gaps having the same relative position within different groups having the same voltage across them. This gives a series of seven identical sets of ten slats. As shown in Fig. 2, the dimensions of the slats are: length $L=80.0$ mm, width (groove depth) $W=30.0$ mm, and thickness $D=1.0$ mm, with the width of the mylar-spaced gaps being $T=75.0$ μm . The repeat distance of the structure is 10.75 mm. To facilitate alignment of the liquid crystal, the aluminium slats are individually coated with a polyimide (AL 1254) film on both sides. They are then baked and the polyimide unidirectionally rubbed, with a soft cloth, along the short axis direction of the slats to provide homogeneous alignment of the liquid crystal director (the average orientation of the long axis of the nematic molecules). The polyimide layers also act as ion barriers preventing ions entering the thin liquid crystal layers when a field is applied. These treated aluminium slats are then stacked as the above array and capillary filled with a nematic liquid crystal (Merck-E7).

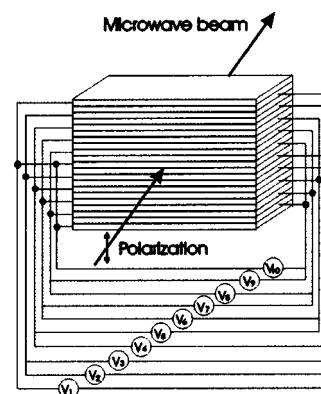


FIG. 1. The grating geometry.

^{a)} Author to whom correspondence should be addressed; electronic mail: j.r.sambles@exeter.ac.uk

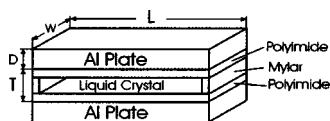


FIG. 2. The structure of a single metallic slit of the grating.

To measure the transmission a horn antenna, fed by a variable frequency microwave generator (50–75 GHz) is set about 80 cm from the grating sample to direct an approximate plane wave normally on to the grating. The zero-order transmitted beam is collected by a second horn antenna that is about 40 cm from the grating and connected to a scalar network analyzer. Because the grating is quite close to the detector horn the grating sample is rotated a little about an axis that is perpendicular to the grating grooves and parallel to the plane of the grating surface (coincident with the polarization direction). This avoids strong interference between the back surface of the grating and the detector horn. Only linearly polarized microwaves are incident with the electric vector lying perpendicular to the groove direction. No transmission is obtained for radiation with its E field along the slit direction. Transmission data were taken as a function of frequency with various combinations of voltages across the liquid crystal-filled gaps. Voltages were selected to give different phases of the microwave outputs at different slats, thus providing, through interference, the potential for output beam steering.

Transmission data as a function of frequency are shown in Fig. 3. The thick solid line corresponds to no voltages applied, the dotted line corresponds to all gaps having voltages of $1.6 V_{\text{rms}}$ and the dashed line corresponds to all gaps having voltages of $3 V_{\text{rms}}$. Finally, the thin solid line in Fig. 3 corresponds to the top six gaps in each group of ten having applied voltages of $3 V_{\text{rms}}$ with the remaining four gaps having applied voltages of $1.6 V_{\text{rms}}$. This particular set of voltages was chosen, as discussed later, to suppress the zero-order transmitted beam at a selected frequency. (Data is normalized with respect to the signal obtained in the absence of the grating.)

From Fig. 3 it is clear that the transmission as a function of frequency has a Fabry-Perot character with modes moving to lower frequency with increasing voltage. Aluminium, at microwave frequencies, has a very large permittivity ($\sim -10^4 + 10^7 i$) and in the narrow gaps ($\sim 75 \mu\text{m}$) coupled SPPs with wave vectors very close to the free space wave vector result.¹⁰ To first order, the coupled SPPs will be reso-

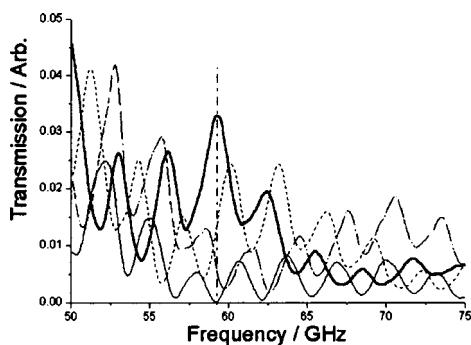


FIG. 3. Transmission data as a function of frequency and applied voltage. For an explanation of the four different lines, see the text. The vertical dotted-dashed line indicates a frequency of 59.2 GHz.

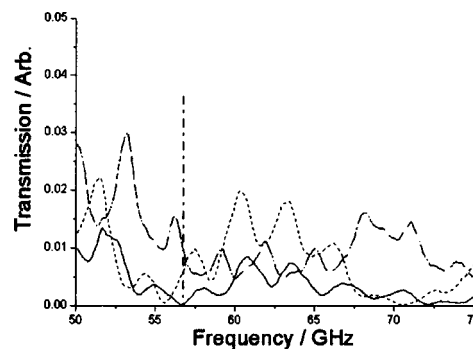


FIG. 4. Transmission data as a function of frequency and applied voltage. For an explanation of the three different lines, see the text. The vertical dotted-dashed line indicates a frequency of 56.7 GHz.

nantly excited when the free space wavelength of the microwave radiation, λ_0 , satisfies¹⁴ $\lambda_0 = 2n \cos \alpha' W/N$, where N is the number of nodes, α' is the internal angle of incidence, and n is the refractive index within the cavity. This type of sample is a “metal-filled” Fabry-Perot, the two highly reflecting surfaces being the front and back surfaces of the aluminium slats.¹¹ The tuning of the resonances arises from the voltage control of the liquid crystal director, as discussed by Yang and Sambles.¹² Increase of voltage causes the director to realign into a homeotropic state, the microwave electric field then experiencing a higher index. Using continuum elastic theory¹⁵ to model the director tilt angle θ distribution through the cell the local effective index is calculated using $n_{\text{eff}} = n_o n_e / (n_e^2 \cos^2 \theta + n_o^2 \sin^2 \theta)^{1/2}$. By integrating across the liquid crystal layer the average effective index as a function of applied field is found. This effective index increases as the applied voltage increases so that for a given mode order, N , the resonant wavelength, λ_0 , increases, i.e., the frequency decreases.

It is apparent that at the frequency of 59.2 GHz (vertical dashed-dotted line in Fig. 3), the signal (thin solid line) drops to zero, while, for no applied voltage across any gap (the thick solid line), the signal is close to maximum. This is explained as follows. Every resonance has a width as shown in Fig. 3. Across each resonant peak different frequencies will have a different phase relative to the center, “resonant,” frequency. 59.2 GHz is at the front edge of the resonant peak corresponding to the dotted line, so it is approximately a $\pi/2$ difference in phase from the central, resonant frequency for every gap having a voltage of $1.6 V_{\text{rms}}$. This frequency is also at the back edge of the resonant peak corresponding to the dashed line. Thus, it has approximately a $\pi/2$ phase difference from the resonant frequency for each gap with $3 V_{\text{rms}}$ applied. Since, for these two cases the two resonance peaks around 59.2 GHz have the same order (with different index values in the cavities), the phase difference of the 59.2 GHz signals from these two different voltage cavities will be $\sim \pi$. In addition, the relative intensity of the two resonances is $\sim 0.62 (= 0.0077/0.0123)$, comparing the $3 V_{\text{rms}}$ with the $1.6 V_{\text{rms}}$ signals as also shown in Fig. 3. So, if in every group of ten gaps a voltage of $3 V_{\text{rms}}$ is established across the top six gaps and a voltage of $1.6 V_{\text{rms}}$ is applied to the remaining four gaps, this will result in two almost equal intensity signals of opposite phase. Destructive interference of these two components results in almost zero transmission at 59.2 GHz. This clearly confirms that this structure acts as a microwave variable phase grating. This is further confirmed by choosing

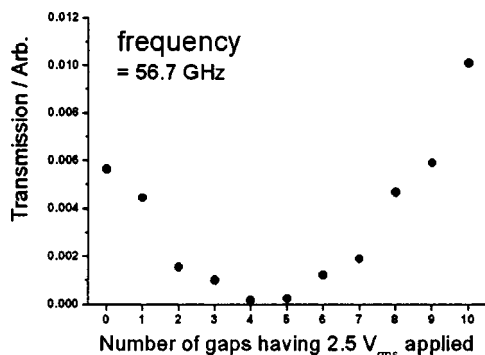


FIG. 5. The transmission at 56.7 GHz against the number of gaps in each group with a voltage of $2.5 V_{\text{rms}}$ (the rest of the gaps in the group have a voltage of $1.5 V_{\text{rms}}$).

different values for the two groups of voltage and applying them across the gaps, with a suitable ratio of the gap numbers in the two groups, then, in principle, the transmission zero may be set at any selected frequency. In Fig. 4 the dotted and dashed lines are for the case of every gap having voltages of $1.5 V_{\text{rms}}$ and $2.5 V_{\text{rms}}$, respectively, and the thin solid line is for the situation when in each group the top four gaps have $2.5 V_{\text{rms}}$ and the remaining six gaps have $1.5 V_{\text{rms}}$. Now the transmission zero point is at 56.7 GHz. It is also apparent that 56.7 GHz, indicated by a vertical dotted-dashed line in Fig. 4, is approximately at the front edge of a dotted line resonance and the back edge of a dashed line resonance, respectively. Furthermore the ratio of the transmission for these two voltage cases is $0.64 (= 0.0062/0.0098)$. Clearly, by varying the ratio of the gaps with the two different voltages, the amount of 56.7 GHz. radiation transmitted is also controlled. This transmission for 56.7 GHz. as a function of the number of gaps having a voltage of $2.5 V_{\text{rms}}$ (the remaining gaps have a voltage of $1.5 V_{\text{rms}}$) is shown in Fig. 5.

Note that with various voltages applied, the grating has a pitch of 10.75 mm. Thus, for our working frequency, higher-order diffracted transmission signals will appear and their intensities may also be controlled by varying the distribution of voltages across the gaps.

In conclusion, by stacking a number of metallic strips with thin gaps between them and filling with aligned liquid crystal, a voltage-controlled variable phase grating at microwave frequencies is demonstrated. Different voltages may be applied independently to each of the ten gaps within a group, with the resulting pattern of voltages repeated in each of the seven groups. For a radiation incident with its electric field polarized orthogonal to the grating grooves, this structure acts as a voltage-controlled phase grating. This is experimentally demonstrated by the fact that the zero-order transmission intensity for any chosen wavelength can be flexibly varied from a maximum to zero by applying appropriate voltages across appropriate gaps.

The authors would like to thank the Engineering and Physical Science Research Council and the Defence Evaluation Research Agency (Farnborough) for their support of this work.

- ¹F. Guerin, J. M. Chappe, P. Joffre, and D. Dolfi, *Jpn. J. Appl. Phys., Part 1* **36**, 4409 (1997).
- ²K. C. Lim, J. D. Margerum, A. M. Lackner, L. J. Miller, E. Sherman, and W. H. Smith, Jr., *Liq. Cryst.* **14**, 327 (1993).
- ³K. C. Lim, J. D. Margerum, and A. M. Lackner, *Appl. Phys. Lett.* **62**, 1065 (1993).
- ⁴K. C. Lim, J. D. Margerum, A. M. Lackner, and E. Sherman, *Mol. Cryst. Liq. Cryst. Sci. Technol., Sect. A* **302**, 187 (1997).
- ⁵T. Thio, H. F. Ghaemi, H. J. Lezec, P. A. Wolff, and T. W. Ebbesen, *J. Opt. Soc. Am. B* **16**, 1743 (1999).
- ⁶T. J. Kim, T. Thio, T. W. Ebbesen, D. E. Grupp and H. J. Lezec, *Opt. Lett.* **24**, 256 (1999).
- ⁷J. A. Porto, F. J. Garcia-Vidal, and J. B. Pendry, *Phys. Rev. Lett.* **83**, 2845 (1999).
- ⁸U. Schroter and D. Heitmann, *Phys. Rev. B* **58**, 15419 (1998).
- ⁹N. P. Wanstall, T. W. Preist, W. C. Tan, M. B. Sobnack, and J. R. Sambles, *J. Opt. Soc. Am. A* **15**, 2869 (1998).
- ¹⁰M. B. Sobnack, W. C. Tan, N. P. Wanstall, T. W. Preist, and J. R. Sambles, *Phys. Rev. Lett.* **80**, 5667 (1998).
- ¹¹H. E. Went, A. P. Hibbins, J. R. Sambles, C. R. Lawrence, and A. P. Crick, *Appl. Phys. Lett.* **77**, 2789 (2000).
- ¹²F. Yang and J. R. Sambles, *Appl. Phys. Lett.* **79**, 3717 (2001).
- ¹³F. Yang and J. R. Sambles, *Phys. Rev. Lett.* **89**, 63901 (2002).
- ¹⁴M. Born and E. Wolf, *Principles of Optics*, 7th ed. (Cambridge University Press, Cambridge, 1999).
- ¹⁵H. J. Deuling, *Mol. Cryst. Liq. Cryst.* **19**, 123 (1972).